J. Fluid Mech. (1980), *vol.* 101, *part* 2, *pp.* 257–279
Printed in Great Britain

The steady flow due to a rotating sphere at low and moderate Reynolds numbers

By S. C. R. DENNIS,
Department of Applied Mathematics, University of Western Ontario, London, Canada

S. N. SINGH
Department of Mechanical Engineering, University of Kentucky, Lexington, U.S.A.

AND D. B. INGHAM
Department of Applied Mathematical Studies, University of Leeds, England

(Received 18 May 1979 and in revised form 4 March 1980)

The problem of determining the steady axially symmetrical motion induced by a sphere rotating with constant angular velocity about a diameter in an incompressible viscous fluid which is at rest at large distances from it is considered. The basic independent variables are the polar co-ordinates (r, θ) in a plane through the axis of rotation and with origin at the centre of the sphere. The equations of motion are reduced to three sets of nonlinear second-order ordinary differential equations in the radial variable by expanding the flow variables as series of orthogonal Gegenbauer functions with argument $\mu = \cos\theta$. Numerical solutions of the finite set of equations obtained by truncating the series after a given number of terms are obtained. The calculations are carried out for Reynolds numbers in the range $R = 1$ to $R = 100$, and the results are compared with various other theoretical results and with experimental observations.

The torque exerted by the fluid on the sphere is found to be in good agreement with theory at low Reynolds numbers and appears to tend towards the results of steady boundary-layer theory for increasing Reynolds number. There is excellent agreement with experimental results over the range considered. A region of inflow to the sphere near the poles is balanced by a region of outflow near the equator and as the Reynolds number increases the inflow region increases and the region of outflow becomes narrower. The radial velocity increases with Reynolds number at the equator, indicating the formation of a radial jet over the narrowing region of outflow. There is no evidence of any separation of the flow from the surface of the sphere near the equator over the range of Reynolds numbers considered.

1. Introduction

The flow due to a sphere rotating with uniform angular velocity about a diameter in a fluid at rest is of intrinsic interest in the fields of meteorology and astrophysics, amongst others, and has received attention both theoretically and experimentally.

0022-1120/80/4574-2400 $02.00

Stokes (1845) and Lamb (1932) considered the problem of a slowly rotating sphere. Here the Reynolds number is small. The Reynolds number can be defined by $R = a^2\omega_0/\nu$, where a is the radius of the sphere, ω_0 its angular velocity and ν the coefficient of kinematic viscosity. Stokes gave the first approximation to the flow and remarked that the sphere behaves like a centrifugal fan causing an inflow to the sphere in the direction of the polar axis and an outflow parallel to the equatorial plane. Bickley (1938) calculated the first-order perturbation in powers of the Reynolds number and found that for small values of R the transition from inflow at the poles to outflow near the equator takes place at an angle $\theta = 54{\cdot}5°$, where (r, θ) are polar co-ordinates in a plane through the polar axis with origin at the centre of the sphere and the initial line coinciding with the polar axis. Further approximations to the solution in powers of R were obtained by Collins (1955), Thomas & Walters (1964) and Ovseenko (1963) and the series has subsequently been extended to eight terms by Takagi (1977), giving the most recent contribution to the low Reynolds number end of the theory.

For large values of R, Howarth (1951) was the first to discuss the laminar boundary layer on a rotating sphere. Howarth showed that in the vicinity of the poles the boundary-layer equations reduce to the von Kármán equations governing the motion of an infinite rotating disk. He obtained an approximate solution of the boundary-layer momentum integral equations by the von Kármán–Pohlhausen method. The problem has subsequently been studied on the basis of boundary-layer theory by Nigam (1954), Stewartson (1958), Fox (1964), Banks (1965, 1976), Manohar (1967) and Singh (1970). A theory which gives the second-order correction to boundary-layer theory has been given by Brison & Mathieu (1973). Experimental studies have been given by Kobashi (1957), Bowden & Lord (1963), Kreith *et al.* (1963) and Sawatzki (1970). In this latter paper measured values of the torque required to rotate the sphere over the range $2 \leqslant R \leqslant 1{\cdot}5 \times 10^6$ were presented together with velocity profiles in both the laminar and turbulent boundary layers. A review of much of the literature prior to that time is given.

The present paper considers the steady axially symmetrical flow due to a rotating sphere in a fluid at rest by the method of series truncation. Early details of this method were given by Van Dyke (1964, 1965). In the present context we are interested in applications to problems involving spherical geometry. Dennis & Walker (1971) considered steady flow past a sphere by this method and Dennis, Walker & Hudson (1973) similarly considered heat transfer from a sphere by forced convection. Brabston & Keller (1975) used the method to study flow past a spherical gas bubble. Munson & Joseph (1971) and more recently Dennis & Singh (1978) applied similar techniques to calculate the flow between two rotating spheres. A comparable method to that used by Dennis & Singh is used in the present paper. Spherical polar co-ordinates (r, θ, ϕ) are used. The motion is independent of ϕ and the Navier–Stokes equations are expressed as three simultaneous second-order partial differential equations governing the stream function, angular velocity and vorticity. These dependent variables are expressed as series of orthogonal Gegenbauer functions with argument $\mu = \cos\theta$, the coefficients of the Gegenbauer functions being functions of the radial variable. Substitution in the Navier–Stokes equations yields three sets of simultaneous ordinary differential equations of the second order which must be solved as functions of the

radial variable. The equations are truncated by setting to zero all terms in the series after a certain stage and the resulting finite sets of equations are solved numerically.

Although the principle of the method is quite similar to that employed by Dennis & Singh (1978), there is one important difference. In the flow between two rotating spheres the range of the radial variable is finite, whereas here it is infinite. Dennis & Singh adopted the modified radial variable $\ln(r/a)$ and the same variable could be used here. However, if either $\ln(r)$ or r itself is used as a variable the problem of approximating the boundary conditions at large distance by boundary conditions at finite values of r has to be considered. Thus in the present paper the variable $\xi = a/r$ is used to make the range of the computations finite. Another reason for adopting this variable is that the perturbation series for small R are polynomials of low degree in ξ with terms involving $\ln(\xi)$ eventually entering in higher approximations together with increasingly higher powers of ξ. Thus finite-difference approximations based on polynomials in the variable ξ are certain to be satisfactory for the lower values of R. The ordinary differential equations are therefore formulated in terms of ξ and boundary conditions are specified at both ends of the range, $\xi = 0$ and $\xi = 1$. Specialized techniques are employed for solving some of the differential equations and, in particular, an integral involving the vorticity is used to calculate values of the vorticity on the sphere. This method was employed by Dennis & Singh (1978) but the principle of the method goes back to papers by Dennis & Chang (1969*a*, *b*, 1970).

Numerical solutions are presented for values of the Reynolds number $R = 1$, 10, 20, 50 and 100. For $R \leqslant 10$, the torque and velocity field characteristics are in good agreement with the series solutions of Collins (1955), Ovseenko (1963) and Takagi (1977), while for $10 \leqslant R \leqslant 100$ the calculated values of the torque agree well with the experimental measurements of Sawatzki (1970) and there is a general tendency in the direction of the boundary-layer results of Howarth (1951) and Banks (1976) for this quantity. The transverse and azimuthal velocity components for $R = 100$ are found to compare reasonably, bearing in mind that the full boundary-layer characteristics have not yet developed, with those measured by Sawatzki (1970) and the theoretical boundary-layer results of Banks (1965). The radial velocity at the equator is found to grow with Reynolds number in a very similar manner to the growth with time found for this quantity by Dennis & Ingham (1979) in the case of the unsteady boundary layer on a sphere which is suddenly started rotating from rest. This seems to be a consequence of the fact that as the Reynolds number increases the region of inflow to the sphere increases and the region of outflow forms a narrowing band near the equator of the sphere due to the collision of the boundary layers. A recent paper by Smith & Duck (1977) suggests that, in situations involving colliding boundary layers such as in the present problem, there is separation from the wall to form a recirculating region whose dimensions are of order $R^{-\frac{3}{14}}$ near the equator. There is no evidence of such a region forming over the range of R considered in the present solutions.

2. Basic equations and analysis

If spherical polar co-ordinates (r, θ, ϕ) are taken with origin at the centre of the sphere and $\theta = 0$ the axis of rotation the motion is independent of the azimuthal angle ϕ. The sphere rotates with angular velocity ω_0 and we can express the motion in terms of dimensionless velocity components (u, v, w) in the directions of r, θ and ϕ,

obtained by dividing the dimensional components (u^*, v^*, w^*) by $a\omega_0$. The dimensional components can be expressed in terms of the stream function ψ^* and the function Ω^* in the form

$$u^* = \frac{1}{r^2 \sin\theta} \frac{\partial \psi^*}{\partial \theta}, \quad v^* = -\frac{1}{r \sin\theta} \frac{\partial \psi^*}{\partial r}, \quad w^* = \frac{\Omega^*}{r \sin\theta}. \tag{1}$$

If we now introduce a dimensionless stream function ψ and dimensionless function Ω given by

$$\psi^* = a^3 \omega_0 \psi, \quad \Omega^* = a^2 \omega_0 \Omega \tag{2}$$

and put $\xi = a/r$ we obtain for the dimensionless velocity components

$$u = \frac{\xi^2}{\sin\theta} \frac{\partial \psi}{\partial \theta}, \quad v = \frac{\xi^3}{\sin\theta} \frac{\partial \psi}{\partial \xi}, \quad w = \frac{\xi \Omega}{\sin\theta}. \tag{3}$$

The Navier–Stokes equations for the motion are easily found to be

$$D^2 \Omega = \frac{R\xi^2}{\sin\theta} \left(\frac{\partial \psi}{\partial \xi} \frac{\partial \Omega}{\partial \theta} - \frac{\partial \psi}{\partial \theta} \frac{\partial \Omega}{\partial \xi} \right), \tag{4}$$

$$D^2 \psi = -\zeta / \xi^2, \tag{5}$$

$$D^2 \zeta = \frac{R\xi}{\sin\theta} \left[\xi \left(\frac{\partial \psi}{\partial \xi} \frac{\partial \zeta}{\partial \theta} - \frac{\partial \psi}{\partial \theta} \frac{\partial \zeta}{\partial \xi} \right) - 2 \left\{ \left(\xi \cot\theta \frac{\partial \psi}{\partial \xi} + \frac{\partial \psi}{\partial \theta} \right) \zeta - \left(\xi \cot\theta \frac{\partial \Omega}{\partial \xi} + \frac{\partial \Omega}{\partial \theta} \right) \Omega \right\} \right], \tag{6}$$

where

$$D^2 = \xi^2 \frac{\partial^2}{\partial \xi^2} + 2\xi \frac{\partial}{\partial \xi} + \sin\theta \frac{\partial}{\partial \theta} \left(\frac{1}{\sin\theta} \frac{\partial}{\partial \theta} \right).$$

The boundary conditions on the surface of the sphere are that

$$\psi = \partial \psi / \partial \xi = 0, \quad \Omega = \sin^2 \theta \quad \text{when} \quad \xi = 1. \tag{7}$$

The fluid at large distances from the sphere is assumed to be at rest so that all the velocity components must vanish as $\xi \to 0$. The appropriate forms of the boundary conditions for Ω, ψ and ζ as $\xi \to 0$ will be considered shortly. The motion is symmetrical about $\theta = \frac{1}{2}\pi$ and hence the region of integration may be taken as

$$0 \leqslant \xi \leqslant 1, \quad 0 \leqslant \theta \leqslant \tfrac{1}{2}\pi$$

subject to the conditions that for all ξ in the given range

$$\Omega = \psi = \zeta = 0 \quad \text{when} \quad \theta = 0, \quad \partial \Omega / \partial \theta = \psi = \zeta = 0 \quad \text{when} \quad \theta = \tfrac{1}{2}\pi. \tag{8}$$

In view of the conditions (8) we may assume the expansions

$$\Omega = \sum_{n=1}^{\infty} I_{2n}(\mu) f_n(\xi), \tag{9}$$

$$\psi = \sum_{n=1}^{\infty} I_{2n+1}(\mu) g_n(\xi), \tag{10}$$

$$\zeta = \sum_{n=1}^{\infty} I_{2n+1}(\mu) h_n(\xi), \tag{11}$$

where $I_n(\mu)$ are the Gegenbauer functions of argument $\mu = \cos\theta$ (Sampson 1891; Happel & Brenner 1965). These functions form a complete orthogonal set in the range $\mu = -1$ to $\mu = +1$ and the terms in the expansions (9)–(11) reflect the correct symmetry properties of the corresponding functions over this range. Substitution of (9)–(11) in the equations (4)–(6) gives rise to infinite sets of ordinary differential equations similar to those given by Dennis & Singh (1978). The least complicated of these sets is that derived from (5), which gives

$$\xi^2 g_n'' + 2\xi g_n' - 2n(2n+1)\, g_n = -\xi^{-2} h_n, \tag{12}$$

where the primes denote differentiation with regard to ξ. This set of equations is obtained by changing variables from θ to μ in (5), substituting (10) and (11) and making use of the orthogonality properties of the functions $I_n(\mu)$.

By the use of similar procedures, (4) and (6) may be reduced to the respective sets of equations

$$\xi^2 f_n'' + 2\xi f_n' - 2n(2n-1) f_n = \xi^2 R_n, \tag{13}$$

$$\xi^2 h_n'' + 2\xi h_n' - 2n(2n+1) h_n = \xi^2 S_n, \tag{14}$$

where the quantities $R_n(\xi)$ and $S_n(\xi)$ are nonlinear combinations of the various functions defined by

$$R_n(\xi) = 2n(2n-1)(4n-1) R \sum_{l=1}^{\infty} \sum_{m=1}^{\infty} \{L(2l-1, 2n-1, 2m) f_l' g_m - L(2m, 2n-1, 2l-1) f_l g_m'\}, \tag{15}$$

$$S_n(\xi) = 2n(2n+1)(4n+1) R \sum_{l=1}^{\infty} \sum_{m=1}^{\infty} [L(2m, 2n, 2l) g_l h_m' - L(2l, 2n, 2m) g_l' h_m + \{2\xi^{-1} L(2m, 2n, 2l) g_l - M(2l, 2m, 2n) g_l'\} h_m - \{2\xi^{-1} L(2l-1, 2n, 2m-1) f_l - M(2l-1, 2m-1, 2n) f_l'\} f_m]. \tag{16}$$

The quantities $L(l, m, n)$ and $M(l, m, n)$ which appear in (15) and (16) are integrals involving products of Gegenbauer functions and derived functions. They are defined by

$$L(l, m, n) = \frac{1}{2} \int_{-1}^{1} \frac{I_{l+1}(\mu)\, I_{m+1}(\mu)\, I_{n+1}'(\mu)}{1-\mu^2}\, d\mu, \tag{17}$$

$$M(l, m, n) = \int_{-1}^{1} \frac{\mu I_{l+1}(\mu)\, I_{m+1}(\mu)\, I_{n+1}(\mu)}{(1-\mu^2)^2}\, d\mu, \tag{18}$$

where the prime in (17) denotes differentiation with respect to μ. It has been shown by Dennis & Singh (1978) that these quantities can be expressed in terms of the Wigner 3-j symbols in the form

$$L(l, m, n) = [lm(l+1)(m+1)]^{-\frac{1}{2}} \begin{pmatrix} l & m & n \\ 1 & -1 & 0 \end{pmatrix} \begin{pmatrix} l & m & n \\ 0 & 0 & 0 \end{pmatrix}, \tag{19}$$

$$M(l, m, n) = \left[\frac{(l-1)(l+2)}{lmn(l+1)(m+1)(n+1)}\right]^{\frac{1}{2}} \begin{pmatrix} l & m & n \\ -1 & -1 & 2 \end{pmatrix} \begin{pmatrix} l & m & n \\ 0 & 0 & 0 \end{pmatrix} - L(l, m, n). \tag{20}$$

Details of the Wigner 3-j symbols are given by Rotenberg *et al.* (1959) and Talman (1968).

The range of the solutions of the sets of ordinary differential equations (12)–(14) is from $\xi = 0$ to $\xi = 1$, where the point $\xi = 0$ corresponds to infinite radial distance from the sphere. The boundary conditions follow from (7) together with the condition that the velocity components must vanish as $r \to \infty$, i.e. as $\xi \to 0$. The boundary conditions for (12) are

$$g_n(1) = g_n'(1) = 0. \tag{21}$$

These are sufficient conditions to determine the set of functions $g_n(\xi)$ from the set of second-order differential equations. No explicit condition is known for $g_n(0)$ since the form of $\psi(\xi, \theta)$ is not known precisely as $\xi \to 0$ except in the case of the perturbation theory valid for small values of R. In the present technique of solution the necessity of assuming a condition for $g_n(0)$ is avoided by devising a special integration procedure in which the set of equations (12) is solved by step-by-step methods. This is a special feature of the present approach to the problem in which it is not necessary to assume an explicit condition for ψ as $r \to \infty$. The boundary conditions for (13) are that

$$f_n(0) = 0, \quad f_n(1) = 2\delta_{n,1} \tag{22}$$

if it is assumed that $\Omega \to 0$ as $\xi \to 0$. The quantity $\delta_{n,1}$ in the second of the conditions (22) is the Kronecker delta. The condition that $\Omega \to 0$ as $\xi \to 0$ is obviously sufficient for w to vanish as $\xi \to 0$ from (3) but it is not a necessary condition. However, it is completely consistent with the solution of Stokes (1845) and is satisfied in all the perturbation solutions in powers of R including the solution consisting of eight terms given by Takagi (1977), so it is assumed to be valid in the present treatment.

The function $\zeta(\xi, \theta)$ must vanish as $\xi \to 0$ but is not known on the surface of the sphere $\xi = 1$ and must be calculated as part of the solution. The boundary conditions for the set of equations (14) may be expressed as

$$h_n(0) = 0, \quad h_n(1) = \alpha_n. \tag{23}$$

The set of constants α_n must be determined and a set of conditions which may be used to do this can be derived from (12). For convenience in subsequent manipulation we make the transformations

$$g_n(\xi) = \xi^{-\frac{1}{2}} G_n(\xi); \quad h_n(\xi) = -\xi^2 r_n(\xi). \tag{24}$$

The set of equations (12) becomes

$$\xi^2 G_n'' + \xi G_n' - k^2 G_n = \xi^{\frac{1}{2}} r_n(\xi), \tag{25}$$

where $k = 2n + \frac{1}{2}$. The boundary conditions for $G_n(\xi)$ are

$$G_n(1) = G_n'(1) = 0. \tag{26}$$

We now multiply (25) by ξ^{k-1} and integrate both sides with respect to ξ from $\xi = 0$ to $\xi = 1$. After some integration by parts of the terms on the left side and then returning to the original variable $g_n(\xi)$ it is found that

$$[\xi^{2n+1}\{\xi g_n'(\xi) - 2n g_n(\xi)\}]_0^1 = \int_0^1 \xi^{2n} r_n(\xi)\, d\xi. \tag{27}$$

The quantity on the left-hand side of (27) vanishes when $\xi = 1$ by (21) and it can also be shown to vanish as $\xi \to 0$. The velocity components (3) must vanish as $\xi \to 0$ and if we substitute in the first two from (10) then

$$\xi^2 g_n(\xi) \to 0, \quad \xi^3 g_n'(\xi) \to 0 \quad \text{as} \quad \xi \to 0. \tag{28}$$

The left-hand side of (27) therefore vanishes for all positive integer values of n and hence

$$\int_0^1 \xi^{2n} r_n(\xi)\, d\xi = 0, \tag{29}$$

for all positive integer values of n. The use of this condition to determine the constants α_n in (23) will be explained in the next section.

The basic problem is now to solve the sets of ordinary differential equations (12)–(14) subject to the conditions (21)–(23), with (29) employed to calculate the unknown values of α_n. The use of (29) is not the only possible procedure for calculating the constants α_n but it is appropriate in the present method, since it is closely linked to the solution of (25) subject to (26) by means of step-by-step procedures. The satisfaction of (29) does in fact ensure that all the boundary conditions are satisfied correctly in the step-by-step integration. The details will be described in the next section, where the solution procedure will be outlined. In the practical numerical integrations the computations must be limited to the determination of a finite number of terms in each of the series (9)–(11) by truncation of the series. A truncation of order n_0 is defined to be the process of setting to zero all terms with subscript greater than n_0 in (9)–(11) and likewise in the sets of differential equations (12)–(14) and solving the resulting set of $3n_0$ second-order differential equations subject to their boundary conditions.

3. Numerical methods

For a given set of constants α_n in (23) both of the sets of differential equations (13) and (14) are coupled sets of second-order differential equations with two-point boundary conditions. The coupling of the equations comes through the dependence of $R_n(\xi)$ and $S_n(\xi)$ on $f_n(\xi)$ and $h_n(\xi)$ according to (15) and (16). The whole set of equations is solved by an iterative procedure, at any given stage of which each equation is considered as a linear differential equation with variable coefficients which depend upon the current values of the various functions involved. We can write a typical equation of either one of the sets (13) and (14) as

$$\xi^2 y_n''(\xi) + \{2\xi + a_n(\xi)\} y_n'(\xi) + b_n(\xi)\, y_n(\xi) = c_n(\xi). \tag{30}$$

Here $y_n(\xi)$ denotes either $f_n(\xi)$ or $h_n(\xi)$. The function $a_n(\xi)$ is the coefficient of the term $y_n'(\xi)$ which has been transferred to the left side of the appropriate equation from either $R_n(\xi)$ or $S_n(\xi)$. Similarly the term $b_n(\xi)$ is made up of the coefficient of the term $y_n(\xi)$ already present on the left-hand side together with the coefficient of a term in $y_n(\xi)$ transferred from either $R_n(\xi)$ or $S_n(\xi)$ as the case may be. Equation (30) can now be approximated by central differences in the form

$$\begin{aligned}[\xi^2 - h\{\xi + \tfrac{1}{2}a_n(\xi)\}]\, y_n(\xi - h) - \{2\xi^2 - h^2 b_n(\xi)\}\, y_n(\xi) \\ + [\xi^2 + h\{\xi + \tfrac{1}{2}a_n(\xi)\}]\, y_n(\xi + h) - h^2 c_n(\xi) = 0\end{aligned} \tag{31}$$

at any typical point of a finite-difference grid, with grid size h, covering the range $\xi = 0$ to $\xi = 1$. For a given function $y_n(\xi)$ the set of equations (31) holds at all internal grid points and thus gives rise to a tridiagonal matrix associated with the values of $y_n(\xi)$ at these points. The most recently available values of $a_n(\xi)$, $b_n(\xi)$ and $c_n(\xi)$ are used in the finite-difference equations (31) at the moment they are solved for a particular function $y_n(\xi)$. The Gauss–Seidel iterative procedure is used to obtain the numerical solution. In this way the whole set of equations of type (30) is solved for the functions $f_n(\xi)$ and $h_n(\xi)$ for $n = 1, 2, \ldots, n_0$ in an over-all iterative sequence until the functions converge to acceptable limits for all values of n. The details are similar to those described by Dennis & Singh (1978).

The main features which need to be described in the present method are the use of the condition (29) and the numerical solution of (25) subject to (26) when (29) has been satisfied. If the range $\xi = 0$ to $\xi = 1$ consists of j grid intervals of length h we can approximate the integral in (29) by a quadrature formula and express the condition approximately as

$$\sum_{i=0}^{j} \lambda_i^{(n)} r_n(ih) = 0, \tag{32}$$

where the coefficients $\lambda_i^{(n)}$ depend upon the quadrature formula used and the factor ξ^{2n} in the integrand has been absorbed in $\lambda_i^{(n)}$. If the sum on the left-hand side of (32) when the term for $i = j$ is omitted is denoted by Q_n it follows that

$$\alpha_n = -r_n(1) = Q_n/\lambda_j^{(n)}, \tag{33}$$

which serves to determine α_n from a knowledge of $r_n(\xi)$, and hence $h_n(\xi)$, at the grid points $\xi = 0, h, 2h, \ldots, 1-h$. In principle any quadrature formula could be used but in practice there is a difficulty if a standard formula such as Simpson's rule is employed. The factor ξ^{2n} in the integrand varies rapidly with ξ if n is large whereas $r_n(\xi)$ itself may not vary rapidly with ξ. Rapid variation of the integrand generally causes a loss in accuracy of the quadrature formula. In the numerical work values of n up to $n = 10$ were used and to avoid the effect of the variation of ξ^{2n} the following method of integration was used.

The range $\xi = 0$ to $\xi = 1$ is divided into pairs of intervals so that j is even in (32). In each pair of intervals $r_n(\xi)$ is approximated by a polynomial of the second degree, following the manner of Simpson's rule. Let ξ_1, ξ_2, ξ_3 denote successive grid points in a given pair of intervals and for convenience let the subscript on $r_n(\xi)$ be suppressed. Then we assume

$$r(\xi) = a + b(\xi - \xi_2) + c(\xi - \xi_2)^2 \tag{34}$$

over the given pair of intervals, where

$$a = r_2, \quad 2bh = r_3 - r_1, \quad 2ch^2 = r_1 - 2r_2 + r_3 \tag{35}$$

and r_1, r_2, r_3 correspond to values of $r(\xi)$ at ξ_1, ξ_2, ξ_3. It follows by a simple integration that

$$\int_{\xi_1}^{\xi_3} \xi^{2n} r(\xi)\, d\xi = \frac{a - b\xi_2 + c\xi_2^2}{2n+1}(\xi_3^{2n+1} - \xi_1^{2n+1}) + \frac{b - 2c\xi_2}{2n+2}(\xi_3^{2n+2} - \xi_1^{2n+2}) + \frac{c}{2n+3}(\xi_3^{2n+3} - \xi_1^{2n+3}). \tag{36}$$

Hence by substitution of the results (35) the integral on the left-hand side of (36) may be evaluated over a typical pair of intervals and thus by summation over all such pairs of intervals the definite integral in (29) is obtained. The coefficient $\lambda_j^{(n)}$ which is needed in (33) is found by applying (36) to the pair of intervals for which $\xi_1 = 1-2h, \xi_2 = 1-h, \xi_3 = 1$ and evaluating the coefficient of $r(1)$. It is thus found that

$$\lambda_j^{(n)} = \frac{1}{2h^2}\left[\frac{(1-h)(1-2h)}{2n+1}\{1-(1-2h)^{2n+1}\}+\frac{3h-2}{2n+2}\{1-(1-2h)^{2n+2}\}\right.$$
$$\left.+\frac{1}{2n+3}\{1-(1-2h)^{2n+3}\}\right]. \quad (37)$$

It follows from this procedure that from grid values of $r_n(\xi)$ at all points other than $\xi = 1$ the satisfaction of (29) determines an approximation to $r_n(1)$ from (33) and then an approximation to $r_n(\xi)$ is known at all grid points. At this stage the numerical solution of (25) subject to (26) may be carried out. This will now be described briefly for a typical equation of the set (25) in which the subscript will be suppressed. The subscript will similarly be omitted from (26). We make the substitutions

$$\xi G' - kG = p, \quad \xi G' + kG = q, \quad (38)$$

and then by (25) $p(\xi)$ and $q(\xi)$ satisfy

$$\xi p' + kp = \xi^{\frac{1}{2}} r, \quad \xi q' - kq = \xi^{\frac{1}{2}} r \quad (39)$$

respectively. It follows from (26) that

$$p(1) = q(1) = 0. \quad (40)$$

To obtain p we integrate the first of (39) in the direction of increasing ξ to get a step-by-step formula. Thus over the three successive points ξ_1, ξ_2, ξ_3 it follows using (36) that

$$p_3 = \beta^k p_1 + \frac{a-b\xi_2+c\xi_2^2}{2n+1}\xi_3^{\frac{1}{2}}(1-\beta^{2n+1}) + \frac{b-2c\xi_2}{2n+2}\xi_3^{\frac{3}{2}}(1-\beta^{2n+2}) + \frac{c}{2n+3}\xi_3^{\frac{5}{2}}(1-\beta^{2n+3}), \quad (41)$$

where $\beta = \xi_1/\xi_3$. The quantities a, b and c are known in terms of r_1, r_2, r_3 from (35) and hence p_3 can be calculated from p_1 and the numerical solution thus advanced two steps at a time.

In order to start the step-by-step procedure from $\xi = 0$ it may be observed that $p(0)$ does not enter the calculation because in the integration of the first of (39) from $\xi = 0$ to any value of $\xi > 0$ the term involving $p(0)$ vanishes under the conditions on $p(\xi)$ implied by (28). This is reflected in (41) by the fact that $\beta = 0$ when ξ_1 coincides with $\xi = 0$. In this way $p(2h)$ can be calculated directly from data involving $r(0)$, $r(h)$ and $r(2h)$ by means of (41). Moreover we can obtain $p(h)$ from the same data by integrating the first of (39) over a single step from ξ_1 to ξ_2 with $\xi_1 = 0$. The result is similar to (41) except that p_3 and ξ_3 must be replaced by p_2 and ξ_2, respectively, and β replaced by $\gamma = \xi_1/\xi_2$. When $\xi_1 = 0$ the value of $p(0)$ clearly does not enter the calculation since $\gamma = 0$. Then $p(\xi)$ may subsequently be calculated at all grid points using (41). Since the condition (29) has been satisfied by summing the right-hand side of (36) for all pairs of intervals, the value of $p(1)$ must come out to be zero to be consistent with the first of (40). This provides a good check on the numerical procedures.

Finally, since $\beta < 1$ in (41) the step-by-step integration is very easily shown to be stable for all values of the grid size.

The integration of the second of (39) by a similar step-by-step method which starts at $\xi = 0$ is easily found to be unstable but since $q(1) = 0$ from (40) we can in this case find a stable method of integration by integrating backwards from $\xi = 1$. In this case it is found that over the same interval $\xi = \xi_1$ to $\xi = \xi_3$

$$q_1 = \beta^k q_3 - \frac{a - b\xi_2 + c\xi_2^2}{2n} \xi_1^{\frac{1}{2}}(1 - \beta^{2n}) - \frac{b - 2c\xi_2}{2n-1} \xi_1^{\frac{3}{2}}(1 - \beta^{2n-1}) - \frac{c}{2n-2} \xi_1^{\frac{5}{2}}(1 - \beta^{2n-2}), \quad (42)$$

where again $\beta = \xi_1/\xi_3$. The formula (42) holds for all $n > 1$ but in the case $n = 1$ the last term must be changed to $+c\xi_1^{\frac{5}{2}} \ln \beta$. Since as before $\beta < 1$ the formula (42), which provides a two-step formula to determine an approximate solution for $q(\xi)$ starting from values of $q(1-h)$ and $q(1)$, is stable. In order to start the integration we need a formula to determine $q(1-h)$. This can be obtained by a modification of (42) in which the integration takes place from $\xi = \xi_2$ to $\xi = \xi_3$. The appropriate formula is obtained by replacing q_1 by q_2 on the left-hand side and ξ_1 and β by ξ_2 and γ, respectively, on the right-hand side. Thus from a given approximation to $r_n(\xi)$ for a given value of n we can obtain approximations to $p_n(\xi)$ and $q_n(\xi)$ by methods which are stable for all values of n. It is found in the calculations that both of these appear to tend smoothly to definite limits as $\xi \to 0$. From the definitions (38) and (24) it then follows that the conditions (28) are satisfied and hence that the velocity components calculated from (3) using (10) tend to zero as $\xi \to 0$.

The sequence of procedures used to obtain a numerical solution for a specified value of R and given values of h and n_0 is substantially that given by Dennis & Singh (1978). From a given starting approximation to all functions and to the boundary conditions α_n in (23) the set of equations (13) is solved for $n = 1, 2, \ldots, n_0$ using the finite-difference analogue (31). This is followed by a similar solution of the set (14). Each set is solved by the Gauss–Seidel procedure; it is quite convenient to perform a fixed number of Gauss–Seidel iterations of (31) corresponding to each differential equation of the sets (13) and (14) rather than completely to solve the set of difference equations (31) to given accuracy before passing to the next equation. The next stage is the calculation of the constants α_n from (33). When this has been performed the set of equations (25) is solved which leads to values of $g_n(\xi)$ and $g_n'(\xi)$ to be used in the calculation of $R_n(\xi)$ and $S_n(\xi)$ from (15) and (16) the next time the sets of equations (13) and (14) are re-solved. This whole iterative procedure is repeated until eventually convergence is achieved. This is decided by the test

$$|\alpha_n^{(m+1)} - \alpha_n^{(m)}| < \epsilon \quad (n = 1, 2, \ldots, n_0). \quad (43)$$

Here ϵ is an accuracy parameter and the superscripts refer to successive estimates during this over-all iterative procedure.

In the course of this iterative procedure the most sensitive feature tends to be the calculation of α_n from (33) and it is necessary to employ an averaging process to determine the next iterate $\alpha_n^{(m+1)}$ from

$$\alpha_n^{(m+1)} = \omega \alpha_n^{(m+\frac{1}{2})} + (1 - \omega)\, \alpha_n^{(m)} \quad (n = 1, 2, \ldots, n_0), \quad (44)$$

R	$h \times 10^2$	n_0	$\epsilon \times 10^4$	ω
1	2·500	4	0·1	0·10
10	1·250	5	0·1	0·10
20	1·250	7	0·1	0·06
50	0·625	10	0·1	0·05
100	0·625	10	0·1	0·03

TABLE 1. Parameters used in the solutions.

where $\alpha_n^{(m)}$ is the previous iterate and $\alpha_n^{(m+\frac{1}{2})}$ is the value obtained from (33). The parameter ω is a relaxation factor whose choice to some extent controls the rate of convergence of the whole process. Generally speaking ω has to be reduced as R increases. One special situation which occurs during the integration of the equations (25) must be mentioned. Although the functions $h_n(\xi)$ satisfy $h_n(0) = 0$, the functions $r_n(\xi)$ defined by (24) do not necessarily vanish as $\xi \to 0$. This may be seen from the form of the solution for low Reynolds numbers which can be written

$$f_1(\xi) \sim 2\xi, \quad g_1(\xi) \sim -\tfrac{1}{4}R(1-\xi)^2, \quad h_1(\xi) \sim -R\xi^2(\tfrac{3}{2}-2\xi) \tag{45}$$

as $R \to 0$, where all functions having subscripts $n > 1$ are $O(R^2)$ at least. Thus

$$r_1(\xi) \sim R(\tfrac{3}{2}-2\xi)$$

in this approximation and is non-zero at $\xi = 0$. Since the values of $r_n(0)$ enter the integration procedure in the general case, the problem is dealt with by assuming that $r_n(\xi)$ can be approximated by a parabola over the two intervals from $\xi = h$ to $\xi = 3h$ and then extrapolating back to $\xi = 0$. This gives the approximation

$$r_n(0) = 3\{r_n(h) - r_n(2h)\} + r_n(3h). \tag{46}$$

This formula was applied repeatedly during the iterative procedure to estimate $r_n(0)$ each time estimates of $r_n(\xi)$ for $\xi \neq 0$ became available following the solution of the set of equations (14).

The calculations were carried out over the range $R = 1$–100. The approximate solution (45) is a good starting assumption for the first truncation ($n_0 = 1$) at small values of R and then at the higher values of R the final solution at the previous R can be used as an initial approximation. Truncations of higher order were carried out for a given value of R by using the results of the previous truncation as a starting assumption and in this way the number of terms in the solution was built up. For small values of R the convergence of the series (9)–(11) is quite rapid and only a few terms are required to describe the properties of the solution quite accurately. As the Reynolds number is increased the number of terms required to give good accuracy also increases. Solutions were carried out for several values of n_0 for each value of R and some judgement was applied as to the maximum value of n_0 required. The solutions were terminated at $R = 100$, when a maximum value of $n_0 = 10$ was necessary. The effect of varying the grid size h was also investigated at different values of R in the range considered. No significant changes in the solution occurred; in fact it is believed that h has been taken generally rather smaller than is necessary. Finally, it was

R	1	2	10
Tagaki (1977)	1·00083	1·0033	1·0745
Present	1·00087	1·0034	1·0736

TABLE 2. Comparison of calculated values of $RM/16\pi$.

necessary to decrease the parameter ω in (44) as R was increased in order to secure convergence of the over-all iterative procedure. The parameters used for each value of R are shown in table 1; the values of n_0 in this table are the largest values used.

4. Calculated results

In the present section the results given are based on the most accurate solutions obtained. These correspond to the parameters given in table 1. We shall start by considering one property of the flow which can be compared with experimental measurements, namely the magnitude of the torque required to rotate the sphere with uniform angular velocity in a fluid at rest. This has been measured for a wide range of R by Sawatzki (1970). Theoretical values have also been given by Collins (1955) and Ovseenko (1963) in terms of series valid for small R and also by Takagi (1977). The torque is given by

$$T^* = \int_{\phi=0}^{2\pi} \int_{\theta=0}^{\pi} r^3 \sin^2\theta \, \tau^*_{\phi r} \, d\theta \, d\phi, \tag{47}$$

evaluated over the surface of the sphere, where $\tau^*_{\phi r}$ is the appropriate component of the stress tensor given by

$$\tau^*_{\phi r} = \rho\nu \left[\frac{1}{r\sin\theta} \frac{\partial u^*}{\partial \theta} + r \frac{\partial}{\partial r} \left(\frac{w^*}{r} \right) \right], \tag{48}$$

and ρ is the density of the fluid. If we substitute (48) in (47) with $\partial u^*/\partial\theta = 0$ on the surface of the sphere we obtain

$$T^* = -2\pi\rho\nu a^3 \omega_0 \int_0^{\pi} \left(\frac{\partial \Omega}{\partial \xi} + 2\Omega \right)_{\xi=1} \sin\theta \, d\theta. \tag{49}$$

Then by substitution of the series (9) for Ω the integral in (49) can be evaluated in terms of $f_1(\xi)$ and its derivative at $\xi = 1$. If we introduce the dimensionless coefficient $M = -T^*/(\frac{1}{2}\rho a^5 \omega_0^2)$ then it is found that, since $f_1(1) = 2$,

$$M = \frac{8\pi}{3R} [4 + f_1'(1)]. \tag{50}$$

The torque is thus dependent only on the derivative at $\xi = 1$ of the first term of (9) and can be calculated quite accurately. The calculated value of $f_1'(1)$ is a function of the order n_0 of the truncation, but this particular quantity converges very rapidly to a limit as n_0 increases. Thus for Reynolds numbers up to 20 the value of M had converged to four significant figures by the time the truncation $n_0 = 4$ was reached. At $R = 50$ it had reached a limit to the same accuracy at $n_0 = 7$ and at $R = 100$ the values were in agreement to four units in the fourth significant figure at $n_0 = 8$ and 10. Some comparison of the present results with those of Takagi (1977) seems worthwhile

R	M	θ_c^0	$R^{-\frac{1}{2}}(\partial\tilde{\zeta}/\partial\theta)_{\xi=1,\theta=0}$	$-R^{-\frac{1}{2}}(\partial\tilde{\zeta}/\partial\theta)_{\xi=1,\theta=\frac{1}{2}\pi}$
1	50·309	54·8	0·249	0·250
10	5·399	58·0	0·645	0·812
20	3·048	62·6	0·642	1·13
50	1·554	69·4	0·583	1·57
100	0·966	73·8	0·568	1·87

TABLE 3. Calculated properties of the solutions.

at small values of R. Takagi gives the first eight terms of the expansion for low Reynolds number in the form

$$\frac{RM}{16\pi} \sim 1+\frac{1}{12}\left(\frac{R}{10}\right)^2-0{\cdot}007\,542\,671\left(\frac{R}{10}\right)^4-0{\cdot}005\,353\,489\left(\frac{R}{10}\right)^6 +0{\cdot}005\,824\,484\left(\frac{R}{10}\right)^8-0{\cdot}003\,398\,21\left(\frac{R}{10}\right)^{10} +0{\cdot}000\,896\left(\frac{R}{10}\right)^{12}+0{\cdot}000\,74\left(\frac{R}{10}\right)^{14}+\ldots, \tag{51}$$

which we have used to calculate the torque in the range $1 \leqslant R \leqslant 10$. The results are shown in table 2, where they are compared with the present results obtained from our most accurate solutions. The agreement is extremely satisfactory bearing in mind that more terms of (51) are probably necessary at $R = 10$.

The results for the torque over the range $1 \leqslant R \leqslant 100$ are given in table 3 along with other properties of the solutions which will be described below. The calculated torque is compared in figure 1 with the experimental results of Sawatzki (1970) and various theoretical results. The curves labelled 1, 2 and 3 correspond to taking the sum of the first one, two and three terms respectively of (51), which give the earlier results of Lamb (1932), Thomas & Walters (1964), Collins (1955) and Ovseenko (1963). The curves labelled 4 and 5 give the results at high Reynolds number

$$M \sim 6{\cdot}48R^{-\frac{1}{2}} \tag{52}$$

and

$$M \sim 5{\cdot}95R^{-\frac{1}{2}}, \tag{53}$$

derived from boundary-layer theory respectively by Banks (1976) and Howarth (1951). The result (51) is not really effective in extending the results derived from the first three terms beyond $R = 10$ and the present results provide some extension of the comparison between experiment and theory in the intermediate range of R. If it is supposed from boundary-layer theory that (52) and (53) give estimates of the leading term of an expansion as $R \to \infty$ whose first two terms are given by

$$M \sim aR^{-\frac{1}{2}}+bR^{-1}, \tag{54}$$

we can estimate a and b by fitting (54) to the calculated values of M at any two large enough values of R. The results of making such estimates for the three pairs of values $R = 10, 20$; $R = 20, 50$; $R = 50, 100$ are shown in table 4. The inference from these results is that

$$M \sim 6{\cdot}45R^{-\frac{1}{2}}+32{\cdot}1R^{-1} \tag{55}$$

as $R \to \infty$.

R	10	20	50	100
a	5·32	6·44	6·45	
b	37·2	32·2	32·1	

TABLE 4. Estimation of the constants in equation (54).

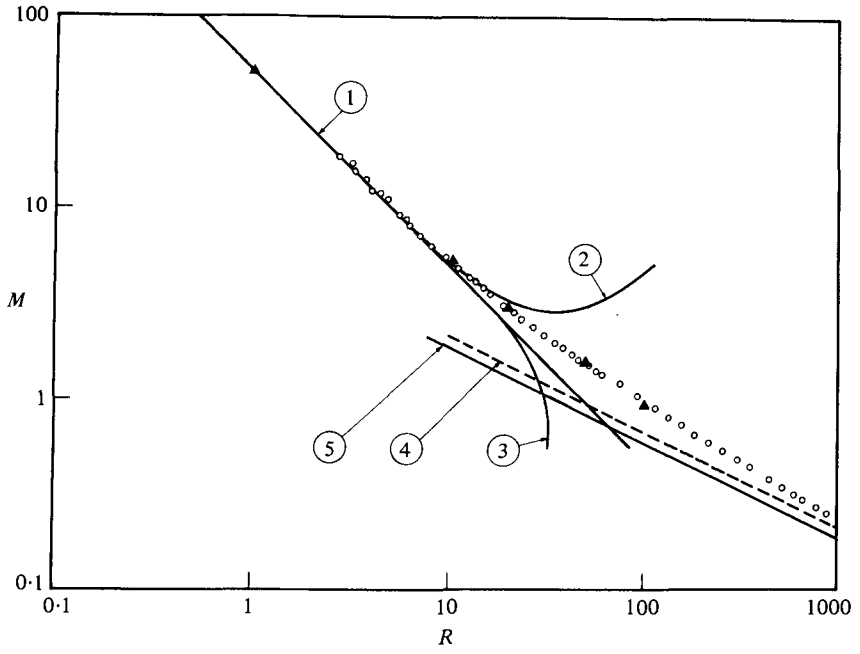

FIGURE 1. Variation of the dimensionless torque $M = -T^*/(\frac{1}{2}\rho a^5\omega_0^2)$ with R. 1, Lamb (1932); 2, Thomas & Walters (1964); 3, Collins (1955) and Ovseenko (1963); 4, Banks (1976); 5, Howarth (1951); ▲, present calculations; ○, experimental measurements of Sawatzki (1970).

The leading coefficient $a = 6{\cdot}45$ in (55) is not only in very good agreement with the estimate (52) of Banks (1976) but also with the estimate $a = 6{\cdot}47$ obtained by Dennis & Ingham (1979) as the limit for large enough time of the unsteady flow due to an impulsively started rotating sphere for large Reynolds number. Results calculated from (55) give an excellent fit with the experimental results of figure 1 over the entire range $20 \leqslant R \leqslant 1000$. No formula of the type (55) derived from second-order boundary-layer theory seems to be available, but Brison & Mathieu (1973) have considered this theory and present calculated results for M graphically over the range

$$10^3 \leqslant R \leqslant 10^5.$$

These agree well with the experimental results of Sawatzki (1970) up to $R = 4 \times 10^4$. Since (55) also agrees well with the experimental observations over the range

$$10^3 \leqslant R \leqslant 4 \times 10^4,$$

it is in good accord with the second-order theory of Brison & Mathieu.

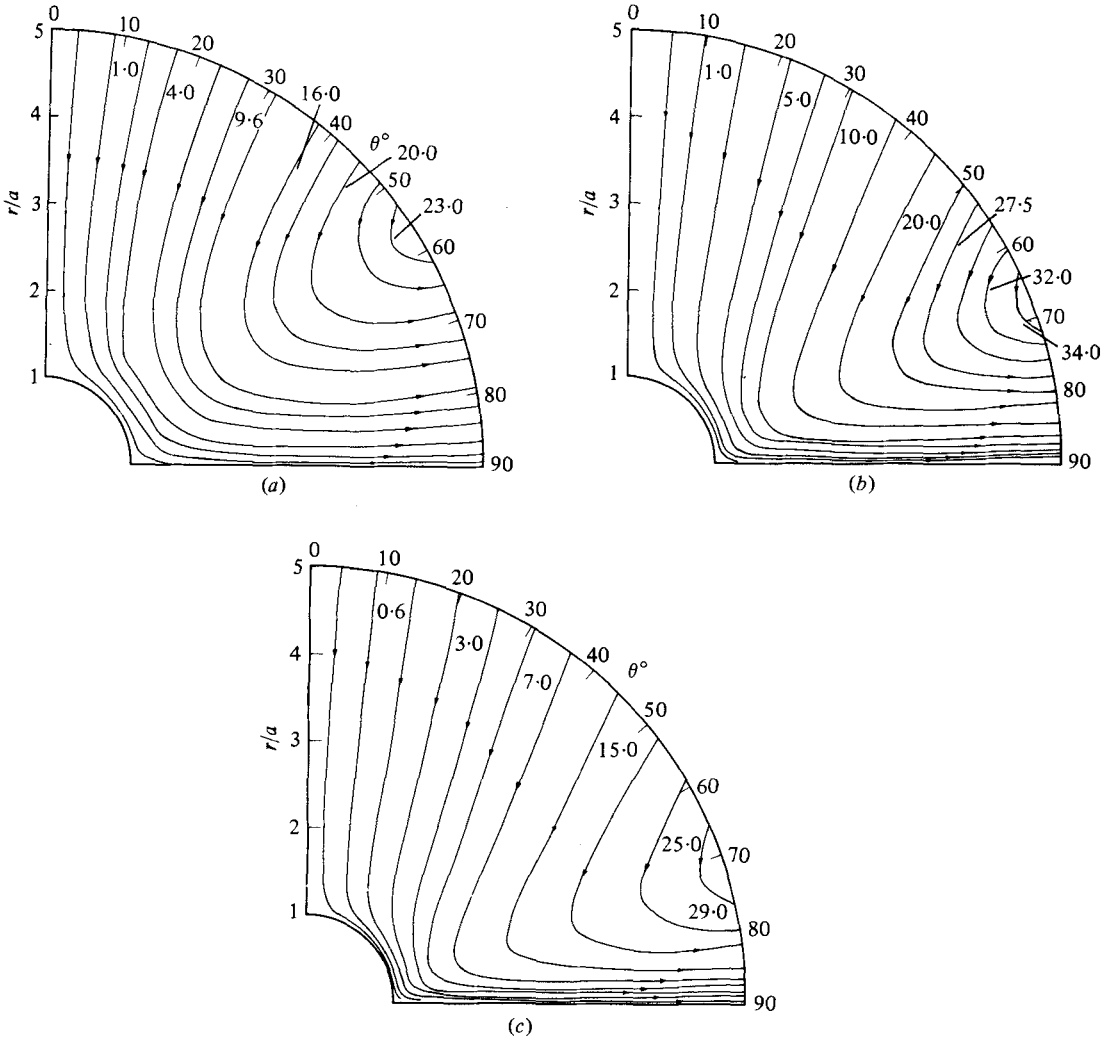

FIGURE 2. Streamlines of the motion for (*a*) $R = 10$; (*b*) $R = 50$; (*c*) $R = 100$. The values to the right of the streamlines are those of -100ψ.

Streamlines of the flow are shown in figure 2. The main feature is the expected inflow at the poles balanced by an outflow at the equator. The inflow changes to an outflow at an angle which depends on R but does not vary greatly with radial distance at fixed R. However, to be precise a definite radial distance has been chosen with which to associate a critical angle $\theta_c(R)$ at which the inflow changes to outflow, nan ~ly that at which the radial velocity component along the equatorial radius $\theta = \frac{1}{2}\pi$ reaches its maximum value. This distance depends upon R and gives a measure of the thickness of the equatorial boundary layer. The variation of $\theta_c(R)$ with R shown in table 3 indicates that the region of inflow increases with R and there is a corresponding decrease of the region of outflow near the equator. The situation with increasing R is in fact similar to the situation which occurs with increasing time at high Reynolds numbers in the development of the unsteady boundary layer on a

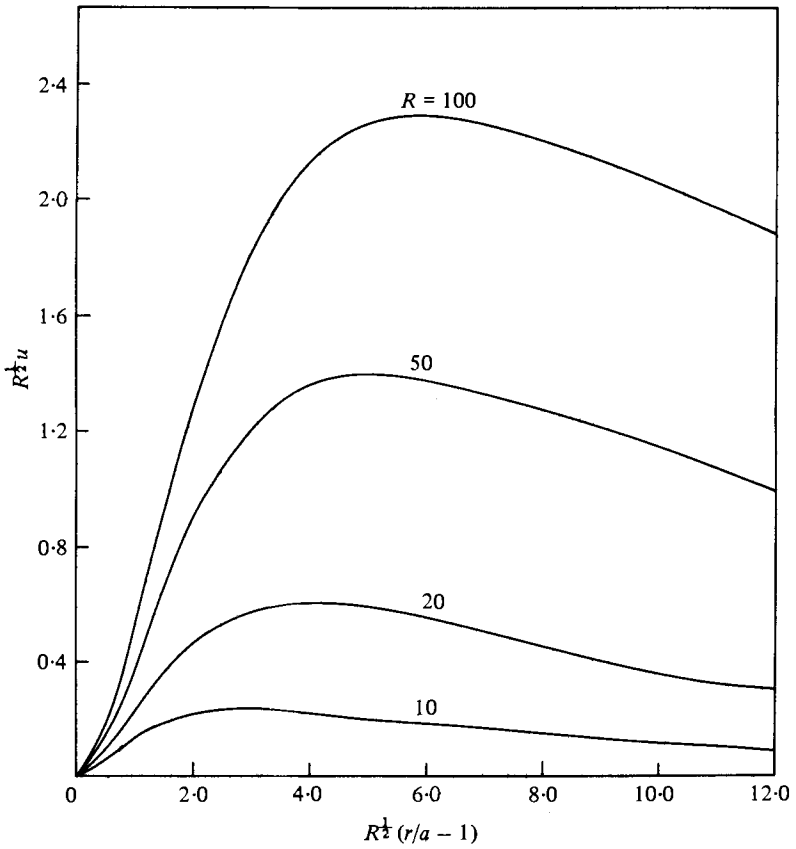

FIGURE 3. Variation of the radial component of velocity with radial distance at $\theta = \frac{1}{2}\pi$ for $R = 10$, 20, 50 and 100.

rotating sphere which was considered by Dennis & Ingham (1979). In that case there was an increase in the radial velocity component at the equator with time. In the present case there is an increase of the radial velocity component with R at the equator; this is shown in figure 3. This increase coupled with the narrowing region of outflow suggests evidence of the formation of the radial jet which has been observed experimentally by Bowden & Lord (1963). The variation of the radial velocity component with radial distance at various stations of θ is shown for the case $R = 100$ in figure 4. The results for lower values of R are somewhat similar with, of course, larger regions of outflow. In every case the radial velocity component tends to zero quite slowly with increasing radial distance; but it does ultimately vanish at large enough values of r.

In figure 5 the vorticity over the surface of the sphere in any plane through the axis of rotation is shown as a function of θ for various values of R. The dimensionless vorticity ξ is related to the function ζ by

$$\xi = \frac{a}{r \sin\theta}\zeta, \tag{56}$$

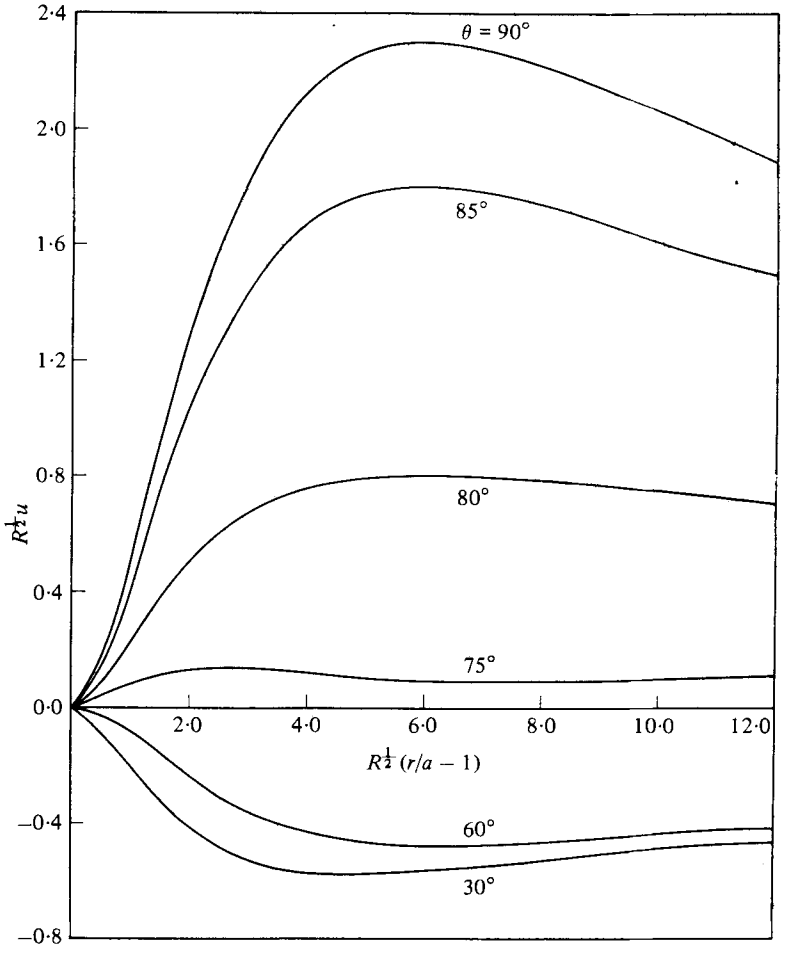

FIGURE 4. Variation of the radial component of velocity with radial distance at various values of θ for $R = 100$.

and may therefore be calculated using the finite number n_0 of terms in the series (11). The main interest of figure 5 is that it indicates that no separation occurs over the surface of the sphere, since $\tilde{\xi} = \partial v/\partial\xi$ on the surface of the sphere and hence a reversal of sign of $\tilde{\xi}$ must take place as a point of separation is passed. Smith & Duck (1977) have given a theory of colliding boundary layers which should be applicable to the present case in which the boundary layers generated at the poles of the sphere collide at the equator to form a jet. In Smith & Duck's theory the collision of the boundary layers is accompanied by separation from the wall to form a re-circulating region of dimension $R^{-\frac{3}{14}}$ which in the present case would occur near the sphere in the equatorial region. There is no evidence of such a region developing in the range of Reynolds numbers considered here. Moreover, the rate of increase of the slope at $\theta = \frac{1}{2}\pi$ of the curves in figure 5 with R indicates that separation is not likely to occur over a considerably larger range of R since not only must the tendency of $\partial\tilde{\xi}/\partial\theta$ at $\theta = \frac{1}{2}\pi$ to increase with R be reversed but it must eventually fall to zero and reverse its sign.

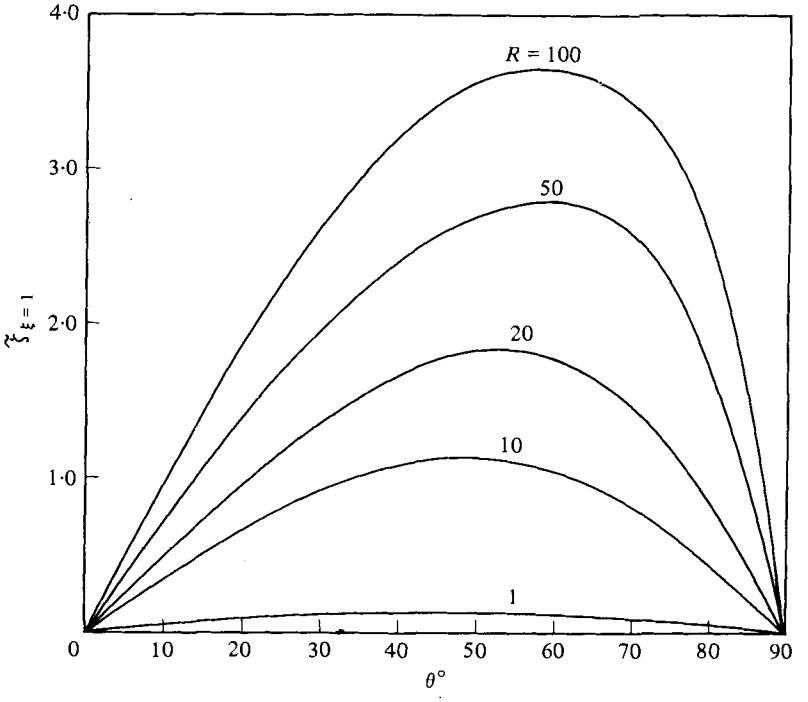

FIGURE 5. Variation of the dimensionless vorticity over the surface of the sphere for $R = 1$, 10, 20, 50 and 100.

The values of $\partial\tilde{\zeta}/\partial\theta$ at $\theta = 0$ and $\frac{1}{2}\pi$ on the surface can be obtained from (56) and (11). It is easily found by use of known properties of the Gegenbauer functions $I_n(\mu)$ that

$$(\partial\tilde{\zeta}/\partial\theta)_{\xi=1,\,\theta=0} = \tfrac{1}{2}\sum_{n=1}^{\infty} h_n(1), \tag{57}$$

$$(\partial\tilde{\zeta}/\partial\theta)_{\xi=1,\,\theta=\frac{1}{2}\pi} = \sum_{n=1}^{\infty} P_{2n}(0)\,h_n(1), \tag{58}$$

where $P_n(\mu)$ is the ordinary Legendre polynomial. The terms in the series on the right-hand side of (57) alternate in sign for each case of R considered and the series converges rapidly for small R but becomes more slowly convergent as R increases. Owing to the alternating nature of the series the sum of a finite number of terms oscillates as each new term is added and it is therefore possible to improve the successive estimates of the sum obtained from m and $m+1$ terms of the series by taking the average of the two sums. This procedure can be extended to the average of the averages and so on and an accurate estimate of the sum thus obtained. In the case of the series on the right of (58) the terms are all of the same sign but the coefficients $P_{2n}(0)$ decrease with n and the convergence of the series is satisfactory for all values of $R \leqslant 100$. Surface values of $\partial\tilde{\zeta}/\partial\theta$ at $\theta = 0$, $\theta = \frac{1}{2}\pi$ are given in table 3. The trend of the values at $\theta = 0$ as R increases could easily be consistent with the result

$$(\partial\tilde{\zeta}/\partial\theta)_{\xi=1,\,\theta=0} \sim 0{\cdot}5102R^{\frac{1}{2}} \quad \text{as} \quad R \to \infty, \tag{59}$$

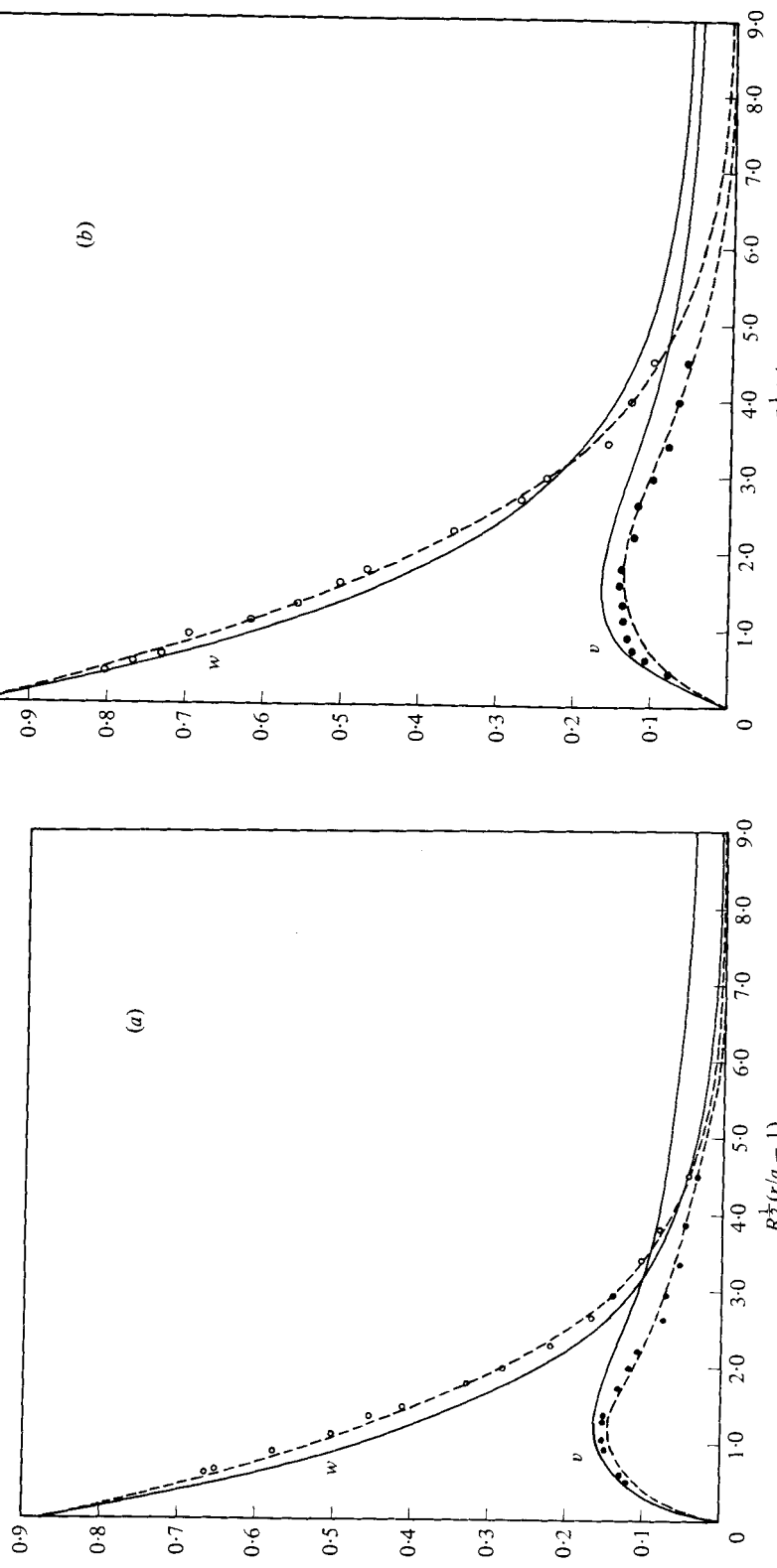

FIGURE 6. Variation of the azimuthal and transverse dimensionless components of velocity at $R = 100$ with radial distance for (*a*) $\theta = 60°$; (*b*) $\theta = 75°$. ——, present calculations; – – –, boundary-layer solution of Banks (1965); ○, experimental measurements of Sawatzki (1970) for w; ●, experimental measurements of Sawatzki (1970) for v.

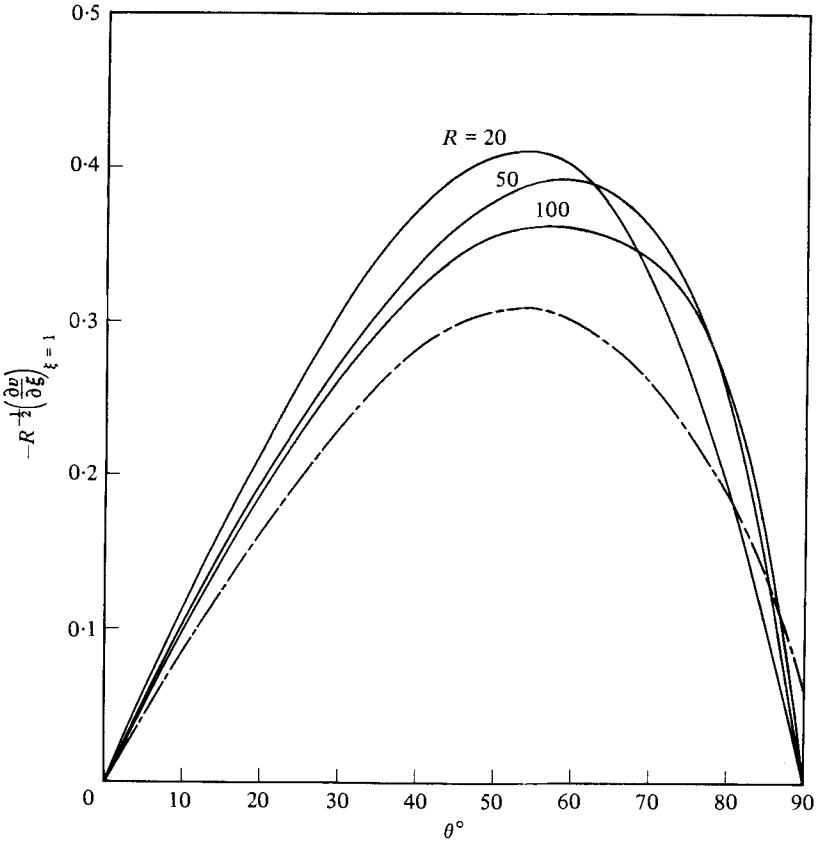

FIGURE 7. Variation of the transverse component of dimensionless skin friction over the surface of the sphere for $R = 20$, 50 and 100. ——, present calculations; – – –, boundary-layer solution of Manohar (1967).

obtained by Banks (1976) from boundary-layer theory. The trend of the values at $\theta = \frac{1}{2}\pi$ merely confirms the trend indicated in figure 5 that a separated region is unlikely to appear near $\theta = \frac{1}{2}\pi$ for other than Reynolds numbers considerably greater than $R = 100$. The theory of Smith & Duck (1977), however, is applicable only in the limit $R \to \infty$.

The characteristics of the flow at $R = 100$ indicate that this Reynolds number is not high enough for the complete characteristics of the boundary-layer theory limit as $R \to \infty$ to appear, but a definite tendency towards the boundary-layer results may be observed; this has already been noted for the torque and the value of $(\partial\tilde{\zeta}/\partial\theta)_{\xi=1,\theta=0}$. In figure 6 the azimuthal and transverse dimensionless components of velocity are shown as functions of radial distance at the two stations $\theta = 60°$ and $\theta = 75°$ at the highest value $R = 100$ computed. They are compared on a boundary-layer scale with the results of Banks (1965) obtained from boundary-layer theory and with the experimental results of Sawatzki (1970) obtained at high Reynolds number. The results are quite similar, bearing in mind that the thickness of the boundary layer is to be expected to be greater at $R = 100$ than that predicted by boundary-layer theory. In figures 7 and 8 the transverse and azimuthal components of the dimensionless skin

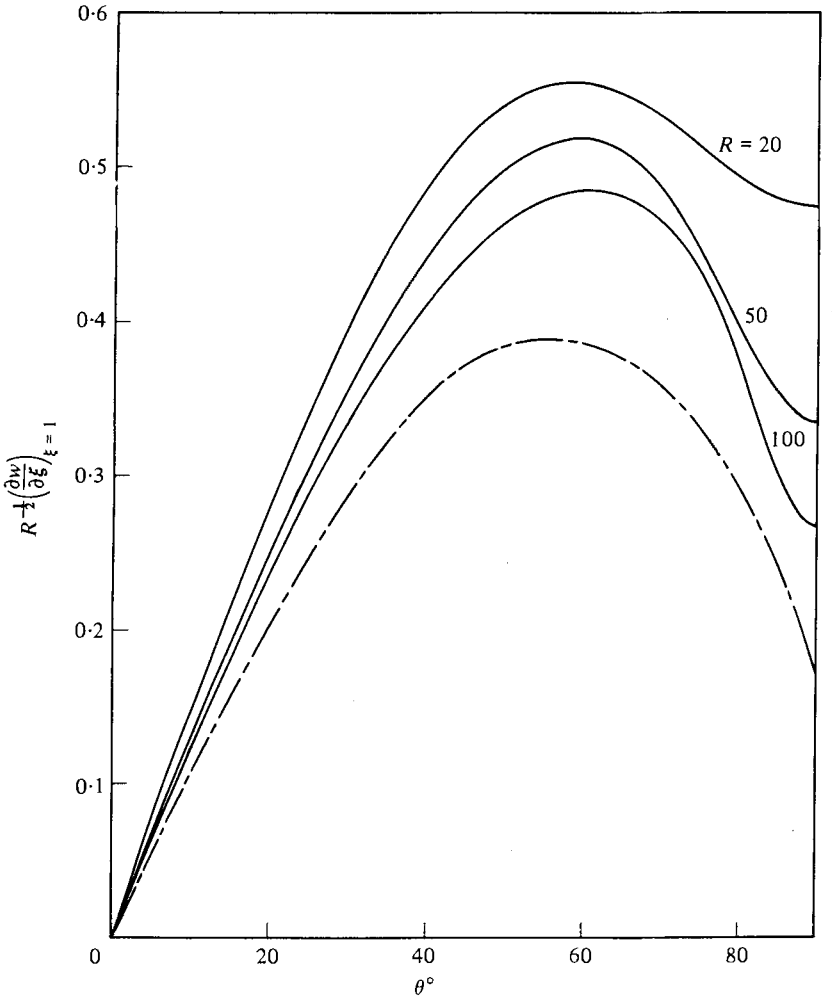

FIGURE 8. Variation of the azimuthal component of dimensionless skin friction over the surface of the sphere for $R = 20$, 50 and 100. ——, present calculations; – – –, boundary-layer solution of Manohar (1967).

friction on the surface of the sphere are given, respectively. It is clear that these components have not approached close to their final limits at $R = 100$ but the general trend is quite consistent with the limiting solutions as $R \to \infty$ obtained from the boundary-layer solution of Manohar (1967), at least over the major portion of the surface measured from $\theta = 0$. It may not be expected that the present solutions of the Navier–Stokes equations will approach the solution of the boundary-layer equations at $\theta = \frac{1}{2}\pi$. The boundary-layer solutions do not satisfy the correct boundary conditions at $\theta = \frac{1}{2}\pi$ since they arise from the solution of parabolic differential equations whose boundary conditions are given only at the pole $\theta = 0$. In the present work the velocity components v and w satisfy the correct conditions $v = 0$, $\partial w/\partial\theta = 0$ at $\theta = \frac{1}{2}\pi$ and this reflects the behaviour at $\theta = \frac{1}{2}\pi$ of the corresponding skin friction components in figures 7 and 8.

The numerical results given in the present section are based on the best approximations available from the computed solutions for each value of R, i.e. those computed with the maximum n_0 and the smallest value of h. Careful checks were applied to the solutions to test their accuracy; for example the solutions were carried out using two grid sizes in several cases. Thus at $R = 50$ solutions were obtained using both $h = \frac{1}{80}$ and $h = \frac{1}{160}$ when $n_0 = 5$. They yielded the values $M = 1{\cdot}5550$ and $M = 1{\cdot}5545$ respectively and other properties compared favourably. The solutions presented are believed to be as accurate as can be obtained by the present method.

The computations were carried out on the CYBER 73 at the University of Western Ontario. The assistance of Mr S. H. Newman with programming and at all stages of the computations is acknowledged. The work formed part of a general project supported by grants from the Natural Sciences and Engineering Research Council of Canada and by NATO.

REFERENCES

BANKS, W. H. H. 1965 *Quart. J. Mech. Appl. Math.* **18**, 443.

BANKS, W. H. H. 1976 *Acta Mechanica* **24**, 273.

BICKLEY, W. G. 1938 *Phil. Mag.* **25**, 746.

BOWDEN, F. P. & LORD, R. G. 1963 *Proc. Roy. Soc.* A **271**, 143.

BRABSTON, D. C. & KELLER, H. B. 1975 *J. Fluid Mech.* **69**, 179.

BRISON, J.-F. & MATHIEU, J. 1973 *C. R. Acad. Sci. Paris* A **276**, 871.

COLLINS, W. D. 1955 *Mathematika* **2**, 42.

DENNIS, S. C. R. & CHANG, G.-Z. 1969*a* *Math. Res. Center, Univ. Wisconsin, Tech. Summary Rep.* no. 859.

DENNIS, S. C. R. & CHANG, G.-Z. 1969*b* *Phys. Fluids Suppl.* **12**, II 88.

DENNIS, S. C. R. & CHANG, G.-Z. 1970 *J. Fluid Mech.* **42**, 471.

DENNIS, S. C. R. & INGHAM, D. B. 1979 *Phys. Fluids* **22**, 1.

DENNIS, S. C. R. & SINGH, S. N. 1978 *J. Comp. Phys.* **28**, 297.

DENNIS, S. C. R. & WALKER, J. D. A. 1971 *J. Fluid Mech.* **48**, 771.

DENNIS, S. C. R., WALKER, J. D. A. & HUDSON, J. D. 1973 *J. Fluid Mech.* **60**, 273.

FOX, J. 1964 Boundary layer on rotating spheres and other axisymmetric shapes. *N.A.S.A.* TN D-2491.

HAPPEL, J. & BRENNER, H. 1965 *Low Reynolds Number Hydrodynamics*, pp. 134–138. Englewood Cliffs, New Jersey: Prentice-Hall.

HOWARTH, L. 1951 *Phil. Mag.* **42**, 1308.

KOBASHI, Y. 1957 *J. Sci. Hiroshima Univ., Japan*, Ser. A **20**, 149.

KREITH, F., ROBERTS, L. G., SULLIVAN, J. A. & SINHA, S. N. 1963 *Int. J. Heat Mass Transfer* **6**, 881.

LAMB, H. 1932 *Hydrodynamics*, pp. 588–589. Cambridge University Press.

MANOHAR, R. 1967 *Z. angew. Math. Phys.* **18**, 320.

MUNSON, B. R. & JOSEPH, D. D. 1971 *J. Fluid Mech.* **49**, 289.

NIGAM, S. D. 1954 *Z. angew. Math. Phys.* **5**, 151.

OVSEENKO, IU. G. 1963 *Izv. Vysshikh Uchevnykh Zavedenii Mathematika* **35**, 129.

ROTENBERG, M., BIVINS, M., METROPOLIS, N. & WOOTEN, J. K. 1959 The 3-*j* and 6-*j* symbols. Massachusetts Institute of Technology Press.

SAMPSON, R. A. 1891 *Phil. Trans. Roy. Soc.* A **182**, 449.

SAWATZKI, O. 1970 *Acta Mechanica* **9**, 159.

SINGH, S. N. 1970 *Phys. Fluids* **13**, 2452.

SMITH, F. T. & DUCK, P. W. 1977 *Quart. J. Mech. Appl. Math.* **30**, 143.

STEWARTSON, K. 1958 In *Boundary Layer Research*, p. 59. Berlin: Springer.
STOKES, G. G. 1845 *Trans. Camb. Phil. Soc.* **8**, 287.
TAKAGI, H. 1977 *J. Phys. Soc. Japan* **42**, 319.
TALMAN, J. D. 1968 *Special Functions*. New York: Benjamin.
THOMAS, R. H. & WALTERS, K. 1964 *Quart. J. Mech. Appl. Math.* **17**, 39.
VAN DYKE, M. D. 1964 *Proc. 11th Int. Cong. Appl. Mech., Munich*, pp. 1165.
VAN DYKE, M. D. 1965 *Stanford Univ.* SUDAER no. 247.